

Electrodeposition of single-crystalline silver pearl chains

Zhe Wu, Hong-Min Li, Xiang Xiong, Guo-Bin Ma, Mu Wang,^{a)} Ru-Wen Peng, and Nai-Ben Ming

National Laboratory of Solid State Microstructures and Department of Physics, Nanjing University, Nanjing 210093, China

(Received 12 October 2008; accepted 23 December 2008; published online 29 January 2009)

We report in this letter the fabrication of unique single-crystalline silver filaments with periodic, pearl-chain-like structures by electrodeposition without using any templates, surfactants, and additives. Fourier transform infrared spectroscopy, infrared focus-plane-array imaging, and numerical simulations demonstrate that the excited surface waves may sustain on the silver “pearl chains” in midinfrared range. Based on the propagation features of surface waves on the silver filaments, we suggest that such a structure can be applied for light transmission in midinfrared range. © 2009 American Institute of Physics. [DOI: 10.1063/1.3072607]

Depending on the frequency of electromagnetic wave, both energy and information can be transmitted by waveguides made of metal or dielectric materials. At optical frequencies an optical fiber can be applied to confine and transfer light, while at microwave frequencies coaxial cables work well.^{1,2} However, neither approach is efficient at far-infrared and terahertz bands because of high loss of metal with finite conductivity and strong absorption of dielectric materials. Recently, a plasmon waveguide based on coupled surface plasmon polaritons (SPPs) among aligned metallic dots has been realized in optical range.^{3–5} It has also been discovered that in terahertz range light can be efficiently transferred along a corrugated metallic wire in a format of spoof SPPs or mimicking SPPs.^{6,7} The dispersion and mode profile of the transmitted light, in this case, are determined by the geometry of the periodic structures on the wire.^{7,8} However, two technical challenges hinder the rapid application of this design. One is that in order to make the periodic corrugated structures on the metal wire, microlithography techniques should be applied, which are usually time consuming and costly. Second, to reduce the loss in transmitting signals, single crystalline metallic materials are preferred, which are not easy to fabricate due to the material anisotropy.

We report in this letter the first fabrication of single-crystalline silver filaments with periodic, pearl-chain-like structure by electrodeposition. Fourier transform infrared (FTIR) spectroscopy and numerical simulations demonstrate that the SPP-like surface waves may sustain on the filaments in midinfrared band, which implies that such kind of structure can serve as a wave-transferring material.

An ultrathin electrodeposition system^{9–11} has been applied to fabricate the microstructured single-crystalline silver filaments without using templates, surfactants, and additives. Similar to our previous design,^{9–11} a Peltier element is placed underneath the electrodeposition cell in order to decrease temperature and to solidify the electrolyte in the cell. During the solidification process, part of the salt in the aqueous electrolyte is expelled from the ice due to the partitioning effect,^{12,13} hence the electrolyte concentration in the solution

increases. When equilibrium is eventually reached at the set temperature ($-4\text{ }^{\circ}\text{C}$, for example), an ultrathin layer of concentrated electrolyte is trapped between the ice of electrolyte and the glass boundary of the electrodeposition cell. The thickness of this layer depends on the temperature and the initial concentration of electrolyte.¹⁰ In our system the typical thickness of this layer is of the order of several hundreds of nanometers. In our experiment, AgNO_3 aqueous electrolyte is prepared by dissolving AgNO_3 (analytically pure, 99.8%) with de-ionized ultrapure water (Millipore, electric resistivity of $18.2\text{ M}\Omega\text{ cm}$) and the concentration is 0.05 M . Parallel, straight electrodes are made of pure silver wire (99.99% pure, 0.5 mm in diameter, Goodfellow) and are sandwiched by two glass slides. The separation of the electrodes is 10 mm . The temperature of the electrodeposition cell is decreased to $-4\text{ }^{\circ}\text{C}$ by a programmable thermostat (Polystat 12108-35, Cole-Parmer). In order to achieve a flat interface of ice of electrolyte, repeated solidification and melting are initially applied until only one or just a few nuclei of ice are left in the system. Thereafter the decreasing rate of temperature is kept at $0.1\text{ }^{\circ}\text{C/h}$ to preserve the flat solid-liquid interface. Eventually a homogeneous, ultrathin layer of concentrated aqueous electrolyte of AgNO_3 can be generated. Potentiostatic electrodeposition is used and the electric voltage is set as 0.3 V . During electrodeposition, silver filaments nucleate from the cathode, develop along the glass substrate, and move toward the anode. The silver electrodeposits are rinsed with ultrapure water and dried in vacuum chamber for further analyses. The morphology and the crystallographic orientations of the silver filaments are characterized by a field emission scanning electron microscope (FESEM) (LEO-1530VP) with electron back scattering diffraction (EBSD) function. For EBSD measurement, a flat plane is milled on the silver pearl chain with focused ion beam (FIB) facility (Strata FIB 201, FEI, 30 keV Ga ions). The reflectance of the silver pearl chains is measured by a FTIR spectrometer (Vertex 70, Bruker) equipped with an infrared microscope with focus-plane-array (FPA) imaging (Hyperion 3000, Bruker).

The silver filaments are silvery shiny in color and consist of pearl-chain-like structure, as shown in Fig. 1(a). The detailed morphology is illustrated in Fig. 1(b). Each “pearl” unit is not exactly identical. In Fig. 1 the average size is

^{a)}Author to whom correspondence should be addressed. Electronic mail: muwang@nju.edu.cn.

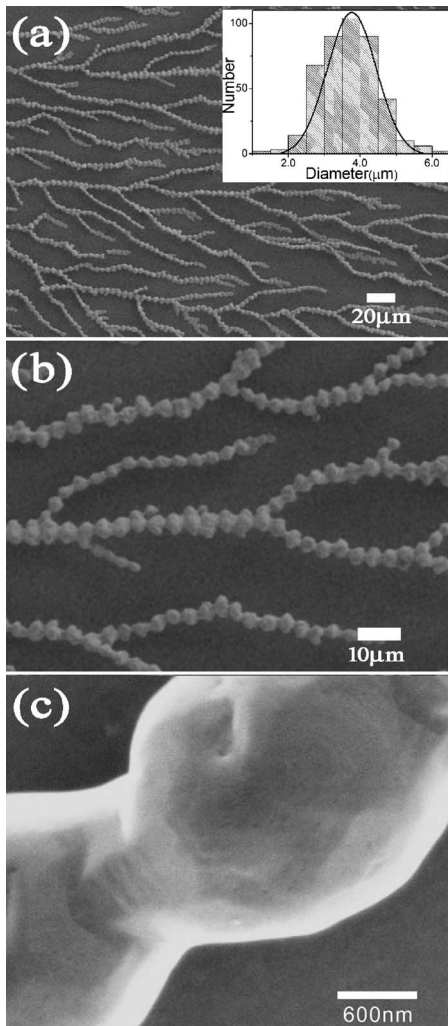


FIG. 1. FESEM micrographs of the silver pearl chains with different magnifications. The filaments are ramified, yet the periodic features on the filament are evident. The inset of (a) shows the distribution of the silver pearl sizes. Some facets can be identified on the surface of the silver pearls (c).

about $3.7 \mu\text{m}$, which can be tuned by the voltage in electrodeposition and the initial concentration of electrolyte solution. Higher magnification indicates that some facets exist on the surface of the silver pearls, as shown in Fig. 1(c), suggesting that they are single crystalline.

The FIB-milled silver filaments are shown in Fig. 2(a), which are observed on a 70° tilted stage in FESEM and some flat cut surfaces can be identified. The filament cross section indicates that the silver filament is compact. The crystallographic orientation of the cut surface marked by the box in Fig. 2(a) is analyzed by EBSD, and the crystallographic orientation is converted into color. As illustrated in Fig. 2(b), the whole cross section of the silver filament possesses the same color, indicating that the whole filament is indeed single crystalline.

Reflectance of the silver-pearl-chain arrays is obtained by FTIR spectrometer associated with an infrared microscope with FPA detector. The resolution of the reflectance spectrum measurements is 4.0 cm^{-1} and the spatial resolution is $2.7 \mu\text{m}$. The numerical aperture of the objective lens ($15\times$) is 0.4, so the divergence angle of the infrared light coming out of the microscope lens is about 46° . This means that when the infrared light shines on the filaments, it has a horizontal component, which plays the role to excite

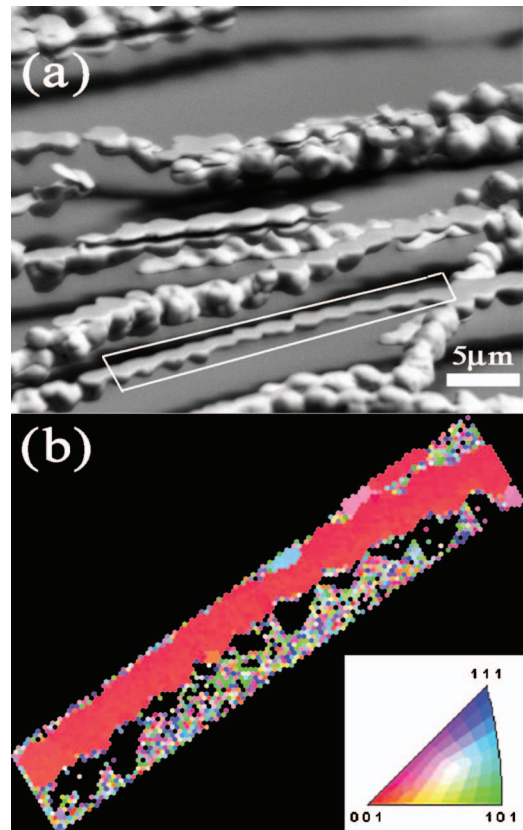


FIG. 2. (Color) (a) FESEM image of the FIB-milled silver pearl chains. Some cut planes can be identified on the filament (the boxed area, for example). (b) EBSD is carried out in the boxed region shown in (a). The color is scaled to the crystallographic orientation. The filament is single crystalline and the cut surface is (001) (in red).

the resonance of SPPs on the structured silver filaments. Figure 3(a) illustrates the optical image of the silver filaments on glass substrate; over this area the infrared spectra are collected. Figure 3(b) shows the reflection spectra of silver

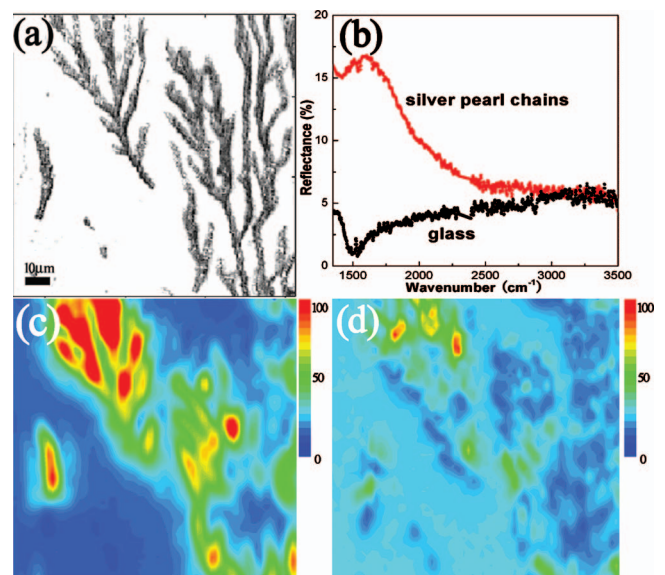


FIG. 3. (Color) (a) The optical micrograph of the filaments of silver pearl chains. (b) Reflectance spectra measured on the silver pearl chains and on the glass substrate, respectively. (c) FTIR FPA imaging of the same region as that shown in (a) with integral region of $1500\text{--}1800 \text{ cm}^{-1}$. (d) FTIR FPA imaging of the same area with integral region of $2900\text{--}3200 \text{ cm}^{-1}$.

filaments and that of the glass substrate, respectively. On the spectrum of the silver filaments, the enhancement of reflectance appears in the range of 1300–2400 cm^{-1} , while in the range of 2400–3500 cm^{-1} , the reflectance of the silver filaments is close to that of the substrate. Figure 3(c) shows the FTIR FPA imaging with integral range of 1500–1800 cm^{-1} . This integral range corresponds to the reflectance-enhanced region as that shown in Fig. 3(b). Although the spatial resolution of FPA detector is low, the correlation of the FTIR imaging in Fig. 3(c) and the morphology of the filaments shown in Fig. 3(a) are easy to identify. Strong intensity distribution occurs on the silver filaments. Figure 3(d) shows the FPA imaging with integral range of 2900–3200 cm^{-1} , which corresponds to the low reflectance region of silver pearl chains in Fig. 3(b). From Fig. 3(d), we cannot clearly identify the shape of the filaments. This suggests that in this frequency range, surface waves cannot go through the silver pearl chains. As a matter of fact, excited by the horizontal component of the incident infrared light, spoof SPP may propagate on the surface of the silver filaments when the frequency is lower than an asymptotic frequency,⁷ which strongly depends on the geometrical structure of the filament. Above the asymptotic frequency, spoof SPP cannot transmit through the filament. In our FPA experiment, the average diameter of the silver pearls is around 2.8 μm and the groove depth is about 1.0 μm . According to Ref. 7, the asymptotic frequency is around 75 THz (2500 cm^{-1}), which is consistent with our observations shown in Fig. 3.

We also apply commercial software (FULLWAVE 4.0) based on finite difference time-domain method to calculate the electric field distribution around an individual silver pearl chain. The diameter and period of the silver pearls were taken as 2.8 and 2.5 μm , respectively. A monotonic Gaussian light shines from the left end of the silver filament and the simulation is carried out in three-dimensional space. In Fig. 4 we plot the electric field distribution on a cross section along the filament axis. It can be seen that around wave number 1681 cm^{-1} , the electric field E propagates along silver pearl chain, and the strong field appears around the silver pearls [Fig. 4(a)]. At larger wave number around 3187 cm^{-1} , the electric field E cannot propagate through the silver pearl chain and the electric field is scattered at the incident site [Fig. 4(b)]. The computer simulations confirm our experimental observations.

For self-organized electrodeposits it remains challenging to control the branching of the metallic filaments. When surface wave propagates along the filament, light scattering is evident at the place where branching occurs. To achieve metallic structures with desired pattern, normally a template is required,¹⁴ and the periodicity can be superimposed by applying external electric pulses.¹⁵ In this way, the propagation of surface waves could be better controlled.

In summary, we report here an easy electrodeposition method to fabricate single-crystalline silver pearl chains. FTIR FPA measurements and numerical simulation show that spoof SPPs can sustain on the silver pearl chains within a certain frequency range. We suggest that such silver pearl chains may have applications for midinfrared detection.

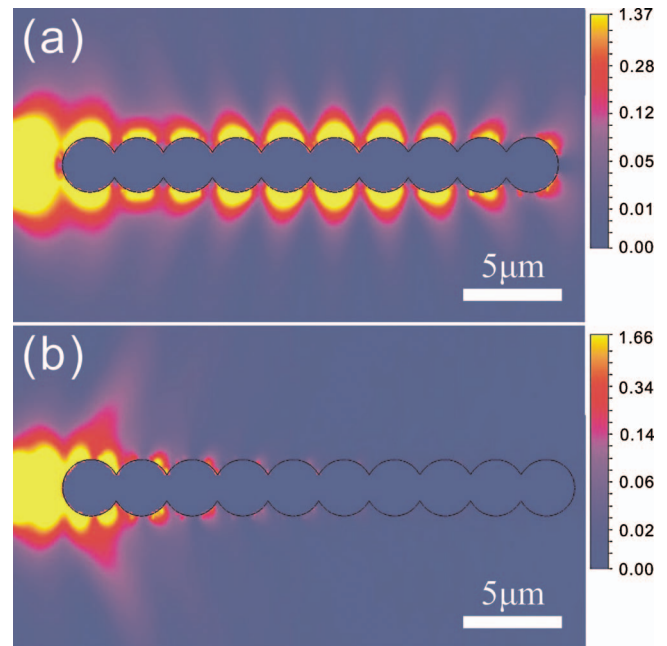


FIG. 4. (Color) Numerical simulation of the electric field distribution on the silver filament with periodic structures. Monotonic Gaussian light with (a) wave number around 1681 cm^{-1} and (b) wave number around 3187 cm^{-1} is introduced from the left end of the silver pearl chain, respectively. In the prior case the light can propagate on the silver pearl chain [as shown in (a)], whereas in the later case, the light cannot go through the chain [as shown in (b)].

The authors gratefully acknowledge the support from the MOST of China (Grant Nos. 2004CB619005 and 2006CB921804), the NSF of China (Grant Nos. 10625417 and 10874068), and Jiangsu Province (Grant No. BK2008012). The assistance of Mr. Ting Wang from Bruker Optics is also acknowledged.

- ¹M. J. Howes and D. V. Morgan, *Microwave Devices: Device Circuit Interactions* (Wiley, New York, 1976).
- ²N. P. Cook, *Microwave Principles and Systems* (Prentice-Hall, Englewood Cliffs, NJ, 1986).
- ³K. B. Crozier, E. Togan, E. Simsek, and T. Yang, *Opt. Express* **15**, 17482 (2007).
- ⁴Q.-H. Wei, K.-H. Su, S. Durant, and X. Zhang, *Nano Lett.* **4**, 1067 (2004).
- ⁵S. A. Maier, M. L. Brongersma, P. G. Kik, and H. A. Atwater, *Phys. Rev. B* **65**, 193408 (2002).
- ⁶J. B. Pendry, L. Martín-Moreno, and F. J. García-Vidal, *Science* **305**, 847 (2004).
- ⁷S. A. Maier, S. R. Andrews, L. Martín-Moreno, and F. J. García-Vidal, *Phys. Rev. Lett.* **97**, 176805 (2006).
- ⁸Y. B. Ji, E. S. Lee, J. S. Jang, and T. I. Jeon, *Opt. Express* **16**, 271 (2008).
- ⁹M. Wang, S. Zhong, X. B. Yin, J. M. Zhu, R. W. Peng, Y. Wang, K. Q. Zhang, and N. B. Ming, *Phys. Rev. Lett.* **86**, 3827 (2001).
- ¹⁰S. Zhong, Y. Wang, M. Wang, M. Z. Zhang, X. B. Yin, R. W. Peng, and N. B. Ming, *Phys. Rev. E* **67**, 061601 (2003).
- ¹¹Y. Wang, Y. Cao, M. Wang, S. Zhong, M. Z. Zhang, Y. Feng, R. W. Peng, X. P. Hao, and N. B. Ming, *Phys. Rev. E* **69**, 021607 (2004).
- ¹²N.-B. Ming, *Fundamentals of Crystal Growth Physics* (Shanghai Science and Technology, Shanghai, 1982).
- ¹³W. Kurz and D. J. Fisher, *Fundamentals of Solidification*, 4th ed. (Enfield, NH, 2001).
- ¹⁴M. Zhang, S. Lenhart, M. Wang, L. Chi, N. Lu, H. Fuchs, and N.-B. Ming, *Adv. Mater. (Weinheim, Ger.)* **16**, 409 (2004).
- ¹⁵B. Zhang, Y.-Y. Weng, X.-P. Huang, M. Wang, R.-W. Peng, N.-B. Ming, B. Yang, N. Lu, and L. Chi, "Creating in-plane metallic nanowire arrays by corner-mediated electrodeposition" (unpublished).